

## Supplementary Information

### **Bifunctional Hydroxyl Group over Polymeric Carbon Nitride to Achieve Photocatalytic H<sub>2</sub>O<sub>2</sub> Production in Ethanol Aqueous Solution with Apparent Quantum Yield of 52.8% at 420 nm**

Weishu Hou,<sup>a</sup> Yunxiang Li,<sup>b,d</sup> Shuxin Ouyang,<sup>\*,a,c</sup> Huayu Chen,<sup>†</sup> Jinhua Ye,<sup>a,b,d</sup> Xiaopeng Han,<sup>e</sup> and Yida Deng<sup>e</sup>

<sup>a</sup>TJU-NIMS International Collaboration Laboratory, School of Materials Science and Engineering, Tianjin University, 92 Weijin Road, Nankai District, Tianjin 300072, China

<sup>b</sup>Graduate School of Chemical Science and Engineering, Hokkaido University, Sapporo 060-0814, Japan

<sup>c</sup>College of Chemistry, Central China Normal University, 152 Luoyu Road, Wuhan 430079, China

<sup>d</sup>Environmental Remediation Materials Unit, International Center for Materials Nanoarchitectonics (WPI-MANA), National Institute for Materials Science (NIMS), 1-1 Namiki, Tsukuba 305-0047, Japan

<sup>e</sup>School of Materials Science and Engineering, Key Laboratory of Advanced Ceramics and Machining Technology of Ministry of Education, Tianjin University, Tianjin 300072, China

\*Author to whom correspondence should be addressed.

Email: [oysx@tju.edu.cn](mailto:oysx@tju.edu.cn); [oysx@mail.ccnu.edu.cn](mailto:oysx@mail.ccnu.edu.cn)

# Contents

Experimental Section.....	3
Figure S1. TEM images of CN and CN-OH samples.....	7
Table S1. Production of H <sub>2</sub> O <sub>2</sub> in different mixtures of water and ethanol over the CN-OH sample.....	8
Table S2. Oxidation products and selectivity of the CN-OH and CN samples....	9
Table S3. Representative CN-based photocatalysts for photocatalytic H <sub>2</sub> O <sub>2</sub> production.....	10
Figure S2. UV-visible absorption spectra of the samples with different amounts of surface hydroxyl group.....	11
Figure S3. Optical properties of the as-prepared samples.....	12
Table S4. Physical properties and H <sub>2</sub> O <sub>2</sub> evolution rate of reference samples....	13
Table S5. Physical properties and H <sub>2</sub> O <sub>2</sub> evolution rate of reference samples with functional groups. ....	14
Supplementary Discussion-1: Main factor influencing photocatalytic activity.	15
Figure S4. Analysis of LSV curves.....	16
Figure S5. Experiments with and without sacrificial reagents.....	17
Table S6. pH values of reference samples before and after reaction.....	18
Figure S6. Cycle test of H <sub>2</sub> O <sub>2</sub> evolution over the CN-OH sample.....	19
Figure S7. Characterizations of the CN-OH sample before and after reaction.	20
Table S7. pH values of each cycle after reaction.....	21
References.....	22

## Experimental Section

### 1. Synthesis of the samples.

The pristine polymeric carbon nitride was prepared by heating melamine with a ramp rate of  $2.5\text{ }^{\circ}\text{C min}^{-1}$  and kept at  $550\text{ }^{\circ}\text{C}$  for 4 h in an  $\text{Al}_2\text{O}_3$  ceramic crucible. The obtained sample was denoted as CN. To synthesize hydroxyl group grafted polymeric carbon nitride, typically, melamine (1.5 g; CP), KCl (7.5 g, AR) and NaOH (varying in the range of 0.00 - 0.15 g; GR) were fully grinded. Then, the mixtures were heated up to  $550\text{ }^{\circ}\text{C}$  with a ramp rate of  $2.5\text{ }^{\circ}\text{C min}^{-1}$  and kept for 4 h. After that, the product was washed fully with distilled water. Finally, the resulting powders were dried at  $80\text{ }^{\circ}\text{C}$  overnight. The final samples were named as CN-OH-x, where  $x = 0.00, 0.01, 0.05, 0.10$  and  $0.15$  corresponding to the weight of added NaOH. The optimized sample synthesized with 0.05 g NaOH was briefly denoted as CN-OH.

For comparison, polymeric carbon nitride with cyano group (CN-cy) was prepared using method as the previous report.<sup>1</sup> A 15 g of urea was dissolved with stirring into aqueous KOH solution (0.1 g in 30 mL  $\text{H}_2\text{O}$ ) and then the resulting solution was dried at  $80\text{ }^{\circ}\text{C}$ . The solid mixture was heated up to  $550\text{ }^{\circ}\text{C}$  with a ramp rate of  $10\text{ }^{\circ}\text{C min}^{-1}$  and kept for 4 h to generate final sample.

### 2. Characterizations

XRD patterns were obtained using a powder X-ray diffractometer (Cu K $\alpha$  radiation source, D8 Advanced, Bruker, Germany). Infrared transmission spectra were obtained with a Fourier transform infrared (FT-IR) spectrophotometer Spectrum (Nicolet 6700, Thermo SCIENTIFIC, America). The diffuse reflectance spectra of the samples were recorded on a UV-visible spectrophotometer (UV-2700, Shimadzu, Japan) with barium sulfate as the reference and then converted into absorption spectra via Kubelka–Munk transformation. Brunauer–Emmett–Teller (BET) surface areas were measured via nitrogen physisorption (Autosorb-iQ2; Quantachrome, America). The electron spin resonance (ESR) measurements were performed on an ESR spectrometer (JES-FA 200, JEOL, Japan). X-ray photoelectron spectroscopy (XPS) measurements were carried out

on XPS instrument (Escalab 250, Thermo SCIENTIFIC, America). Field Emission Scanning Electron Microscope (S4800, HITACHI, Japan) and Transmission Electron Microscope (Tecnai G2 F20, FEI, Holland) were used to obtain the microstructure of the samples.

### 3. Photocatalytic Reactions

#### 3.1 Photocatalytic $H_2O_2$ production

The photocatalytic  $H_2O_2$  production ability of the samples were evaluated by the reduction of molecular oxygen. The schematic diagram of the photocatalytic  $H_2O_2$  production process was shown in Figure S1. For these experiments, 40 mg photocatalyst was suspended in 40 ml solution containing 25 mL of purified water and 15 mL of ethanol. Before the irradiation, the suspension was stirred under artificial air [V ( $O_2$ ): V ( $N_2$ ) = 1: 4] purging for 30 min in dark to make it  $O_2$ -saturated. The reactor was irradiated by a 300 W Xe lamp equipped with a L42 cutoff filter ( $\lambda > 400$  nm) with continuous stirring and purging. During the irradiation, about 3 mL of suspensions were sampled and filtered in every 10 min duration to remove the suspended photocatalyst. The amount of  $H_2O_2$  generated was determined by performing a redox titration against  $KMnO_4$  reagent.

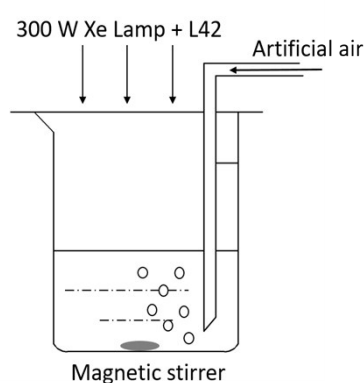


Figure SI-1. Schematic diagram of the photocatalytic  $H_2O_2$  production.

The recycling tests were performed as follows. After the first cycle, the suspension was washed by centrifugation, dried overnight and then redispersed in the solution. The

same procedure was repeated up to a fifth cycle.

### 3.2 Quantum yields

In the cases of the measurement of apparent quantum yield (AQY), a 420 nm band-pass filter and a L42 cutoff filter were used to produce monochromatic light. The intensity of incident light was measured by a spectroradiometer (AvaSolar-1, Avantes, America). The amount of evolved H<sub>2</sub>O<sub>2</sub> was analyzed by DPD method.<sup>2</sup> The light intensity at 420 nm was measured as 15.87 μmol/(s•m<sup>2</sup>) and the irradiation area was 16.62 cm<sup>2</sup>. AQY was estimated according to following equation:

$$\text{AQY} = N(\text{H}_2\text{O}_2) \times 2 / N(\text{Photons}) \times 100\%$$

in which N (H<sub>2</sub>O<sub>2</sub>) and N (Photons) referred to the molecular number of generated H<sub>2</sub>O<sub>2</sub> in unit time and the number of incident photons in unit time, respectively. In the photocatalytic H<sub>2</sub>O<sub>2</sub> production of present study, we have proved that the reduction of O<sub>2</sub> into H<sub>2</sub>O<sub>2</sub> goes through a sequential two-step single-electron O<sub>2</sub> reduction route, which means that one molecule of H<sub>2</sub>O<sub>2</sub> generation will consume two photoelectrons, thereby the number of used photons equals to the number of generated H<sub>2</sub>O<sub>2</sub> multiplied by a factor of 2.

### 3.3 Rate of CH<sub>3</sub>CHO formation

As for the photocatalytic rate of CH<sub>3</sub>CHO formation and selectivity of the samples, the pretreatment of the samples were the same as the photocatalytic H<sub>2</sub>O<sub>2</sub> evolution except that it was carried out in a 500 ml sealed cell (Figure S2). Before irradiation, the cell was purged with artificial air for 10 min to remove the CO<sub>2</sub> gas. During the irradiation, about 0.2 μL of the suspension and 0.5 ml of the gas were sampled and the amount of CH<sub>3</sub>CHO and CO<sub>2</sub> generated were determined by gas chromatograph (GC-2014, Shimadzu Corp., Japan) equipped with a FID detector and methanizer. The byproduct of CH<sub>3</sub>COOH was detected on a 500 MHz nuclear magnetic resonance (NMR, Varian INOVA, America).

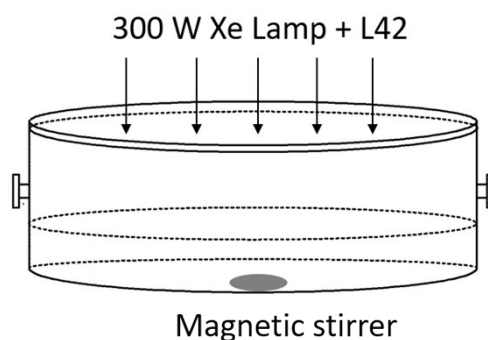


Figure SI-2. Schematic diagram of the photocatalytic rate of  $\text{CH}_3\text{CHO}$  formation.

#### 4. Electrocatalytic Measurements

A PARSTAT 4000 electrochemical workstation (AMETEK) was employed to perform the electrochemical measurements in a conventional three-electrode test cell with sample-modified glassy carbon as the working electrode, a saturated calomel electrode (SCE) as the reference electrode and a platinum plate as the counter electrode, respectively. To obtain catalyst slurries, 15 mg of the sample and 80  $\mu\text{L}$  Nafion solution were dispersed in 1.5 mL solution containing 0.7 mL of purified water and 0.8 mL of ethanol by sonication to form a homogeneous ink.

As for the working electrode, the glassy carbon (GC) electrode was polished sequentially with aqueous slurries of 0.3 and 0.05 mm alumina powders on a polishing microcloth. Then 10  $\mu\text{L}$  of the catalyst slurries were drop-coated on the rotation ring electrode (RDE) (diameter = 5 mm). The ORR was tested in  $\text{O}_2$ -saturated 0.1 M KOH. The cyclic voltammetry (CV) curves were measured from 0.2 to 1.1 V versus RHE for ORR at a scan rate of 20  $\text{mV s}^{-1}$ . The potential was calibrated to versus RHE according to following equation:

$$E (\text{vs. RHE}) = E (\text{vs. SCE}) + 0.059 \times \text{pH} + 0.241 \text{ V}.$$

The RDE was scanned cathodically with varied rotating speed at 400, 600, 900, 1200, 1600, 2000 round per minute (rpm), respectively.

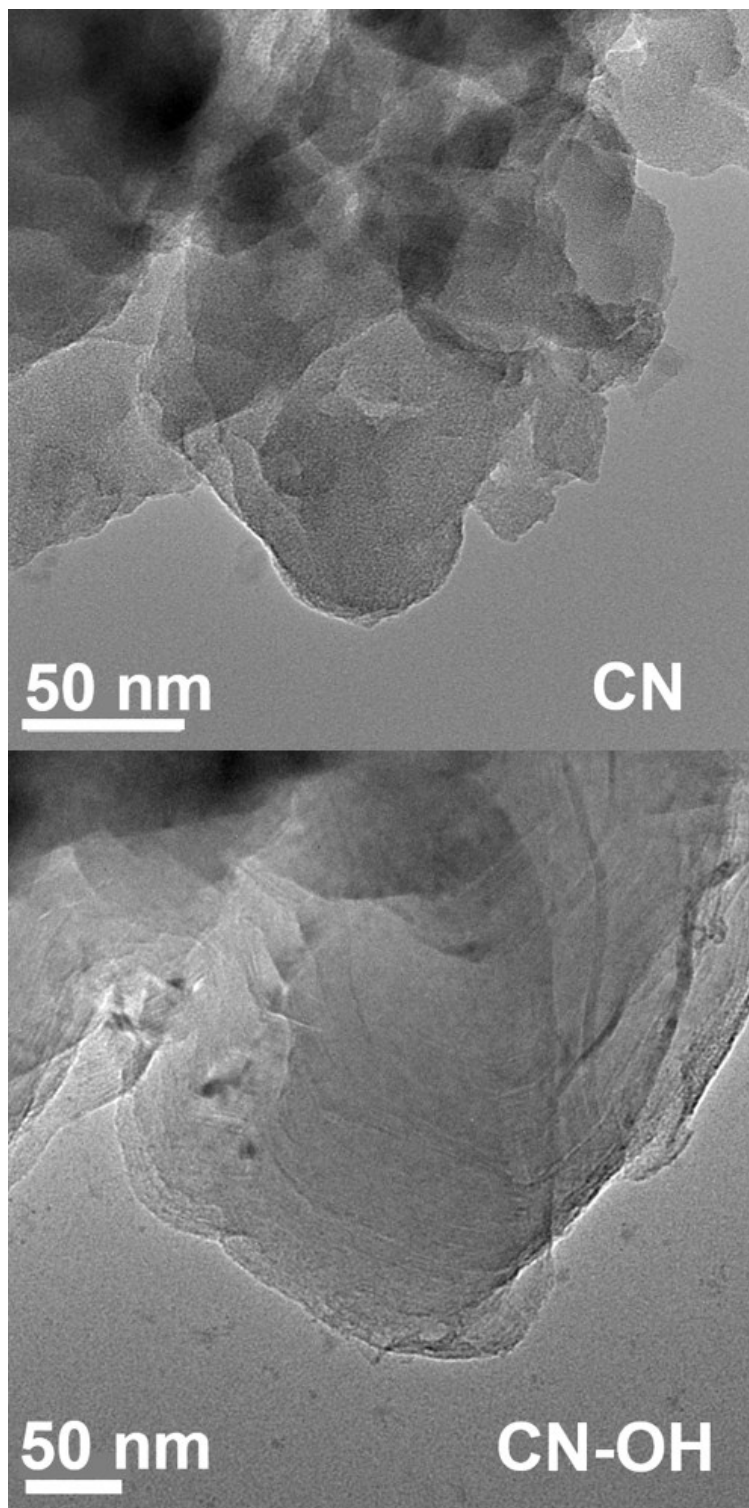


**Figure S1. TEM images of CN (top) and CN-OH (bottom) samples.**

**Table S1. Production of H<sub>2</sub>O<sub>2</sub> in different mixtures of water and ethanol over the CN-OH sample**

(Photocatalytic reaction conditions: 40 mg of catalyst, 40 ml of water and ethanol mixture, 300 W Xe lamp with a L42 cutoff filter,  $\lambda > 400$  nm)

The amount of ethanol added (ml)	5	10	15	25	40
H <sub>2</sub> O <sub>2</sub> ( $\mu$ mol/h)	404	610	728	726	705

**Table S2. Oxidation products and selectivity of the CN-OH and CN samples**

	H <sub>2</sub> O <sub>2</sub> ( $\mu$ mol)	CO <sub>2</sub> ( $\mu$ mol)	CH <sub>3</sub> CHO ( $\mu$ mol)	CH <sub>3</sub> CHO Selectivity (%)
CN	3.0	0.2	7.2	95.97
CN-OH	183.7	0.1	277.1	99.95

**Table S3. Representative CN-based photocatalysts for photocatalytic H<sub>2</sub>O<sub>2</sub> production**

Samples	Product yield (μM/h)	Light Source	Reaction Conditions	AQY at 420nm
KPD-CN-7.5 <sup>3</sup>	243	300W Xe lamp λ > 420 nm	0.5 g/L O <sub>2</sub> 10 vol% of ethanol	8.0%
OCN-500 <sup>4</sup>	2920	300W Xe lamp λ >420 nm	1 g/L O <sub>2</sub> 10 vol% of isopropanol	10.2%
g-C <sub>3</sub> N <sub>4</sub> -SiW <sub>11</sub> <sup>5</sup>	152	300W Xe lamp AM 1.5	1 g/L O <sub>2</sub> 5 vol % methanol	6.5%
DCN-15A <sup>6</sup>	81	AM1.5 λ > 420 nm	0.83 g/L O <sub>2</sub> 20 vol % of isopropanol	10.7%
KPF_CN <sup>7</sup>	333	300W Xe lamp λ >420 nm	0.5 g/L O <sub>2</sub> 10 vol% of ethanol	24.3%
<b>This Work</b>	<b>18200</b>	<b>300W Xe lamp</b> <b>λ &gt;400 nm</b>	<b>1 g/L air</b> <b>38 vol % of ethanol</b>	<b>52.8%</b>

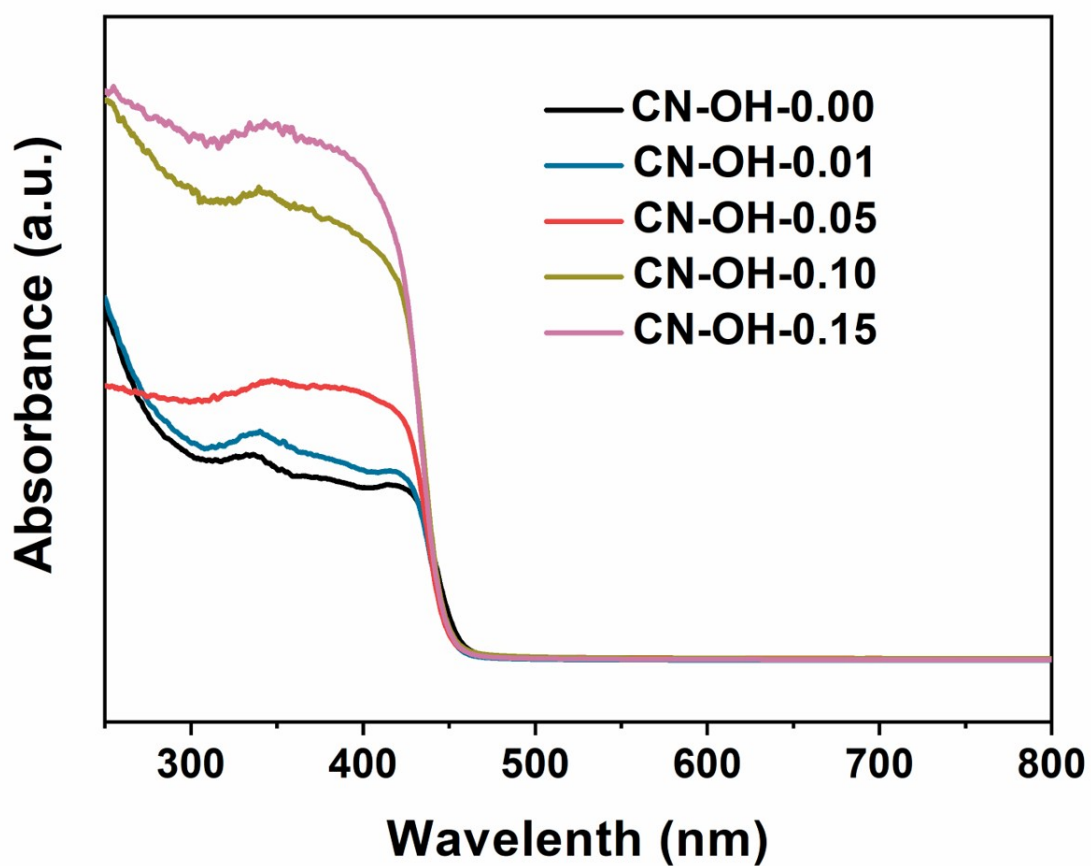


Figure S2. UV-visible absorption spectra of the samples with different amounts of surface hydroxyl group.

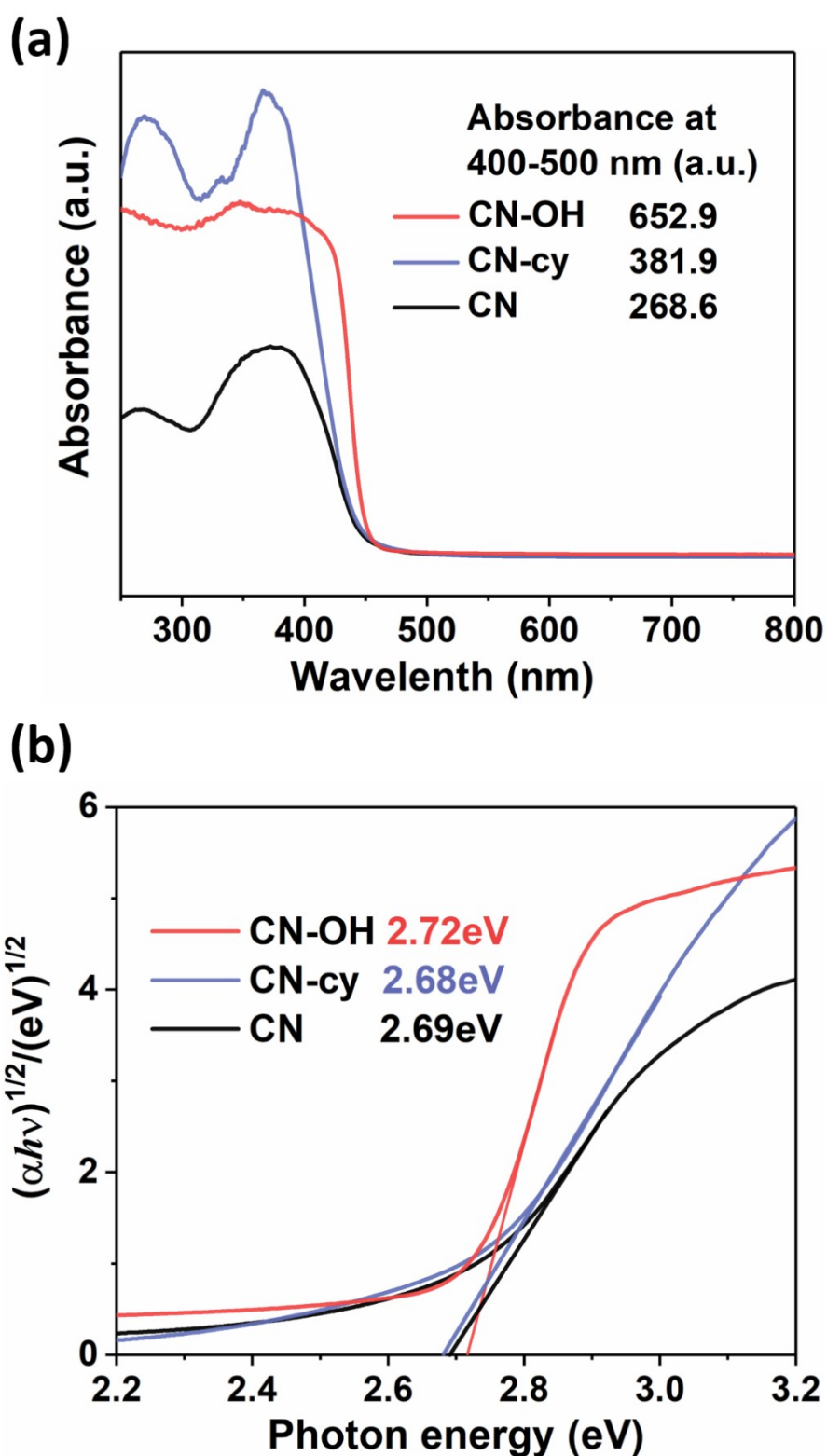


Figure S3. Optical properties of the as-prepared samples. (a) UV-visible absorption spectra and (b) the plots of the  $(\alpha hv)^{1/2}$  versus photon energy ( $hv$ ) over the CN, CN-cy and CN-OH samples.

**Table S4. XRD peak FWHM, surface area and H<sub>2</sub>O<sub>2</sub> evolution rate of reference samples**

	XRD peak FWHM	surface area (m <sup>2</sup> /g)	H <sub>2</sub> O <sub>2</sub> evolution rate (μmol/h)
CN	1.37	9.9	13
CN-OH-0.00	0.61	7.9	206
CN-OH-0.01	0.66	14.5	511
CN-OH-0.05	0.66	66.5	728
CN-OH-0.10	0.78	75.2	622
CN-OH-0.15	0.74	76.6	492

**Table S5. XRD peak FWHM, surface area and H<sub>2</sub>O<sub>2</sub> evolution rate of reference samples with different functional groups**

	XRD peak FWHM	surface area (m <sup>2</sup> /g)	H <sub>2</sub> O <sub>2</sub> evolution rate (μmol/h)
CN	1.37	9.9	13
CN-cy	1.37	49.6	39
CN-OH	0.66	66.5	728

### **Supplementary Discussion-1: main factor influencing photocatalytic activity**

The photocatalytic activity is affected by several factors such as light absorbance, surface area, crystallinity, active sites and so on. To identify the main factor, more reference samples have been fabricated and their physical properties and photocatalytic activities are listed in Table S4. The CN-OH-0.05 sample possesses lower light absorbance than CN-OH-0.15 (Figure S1) but delivers an improved H<sub>2</sub>O<sub>2</sub> evolution, suggesting that light absorbance is not the main factor. The surface area of CN-OH-0.05 is about 4.5 times higher than that of CN-OH-0.01; however, the photocatalytic H<sub>2</sub>O<sub>2</sub> generation is 1.4 times higher, revealing the surface area is not the dominant factor. As for the crystallinity, CN-OH-0.01 is better than that of CN-OH-0.10, but CN-OH-0.10 shows better photocatalytic H<sub>2</sub>O<sub>2</sub> activity, indicating the crystallinity is excluded. Probably, the functional groups act as active sites which are crucial to the reaction. Because the cyano group was introduced as an accompanied functional group in the present synthesis, the reference sample with individual cyano group grafting (CN-cy) was also prepared. The basic physical properties of CN-OH and CN-cy (Table S5 and Figure S2) didn't show too much difference, whereas CN-OH shows notable promotion of photocatalytic activity. Thus it is rational to infer that OH groups rather than cyano groups take crucial effect on enhancing photocatalytic performance.

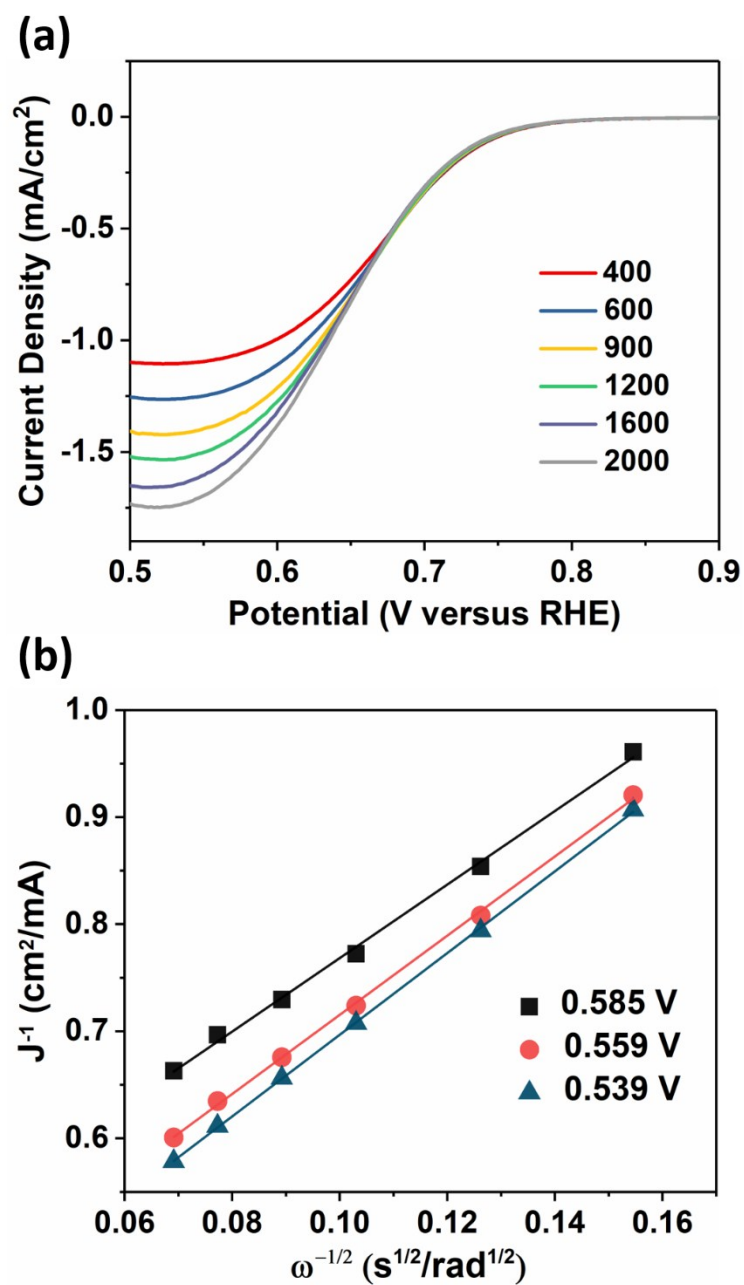
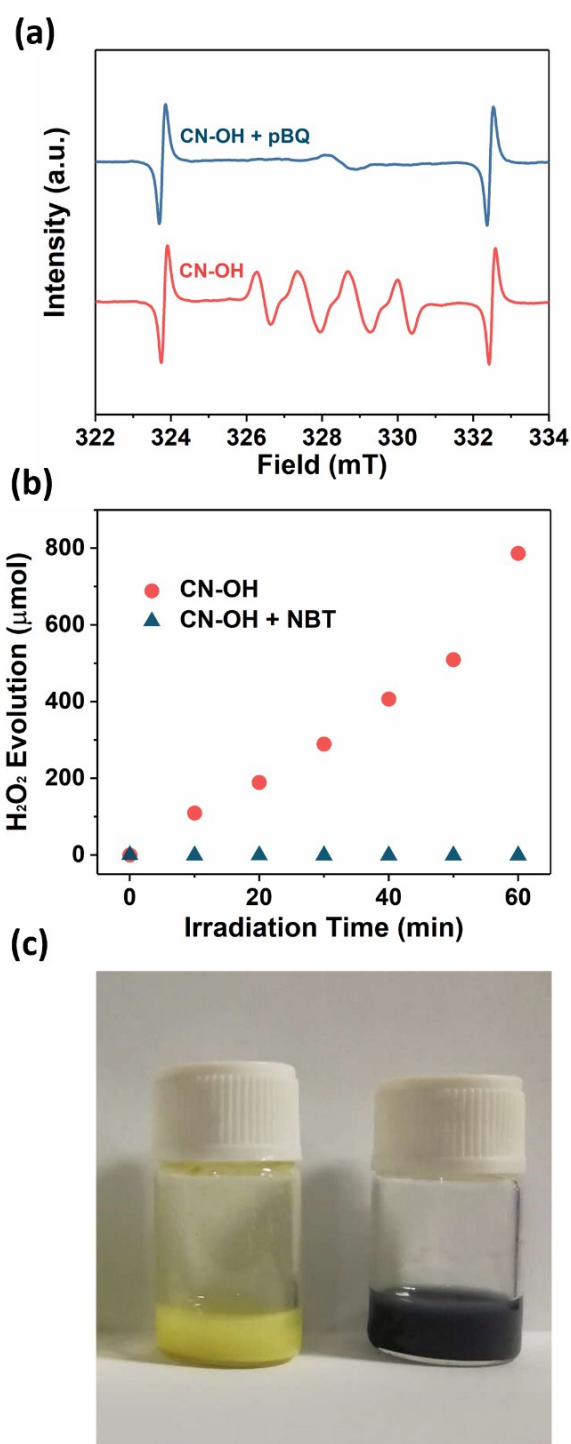


Figure S4. Analysis of LSV curves. (a) Rotating-disk voltammograms and (b) corresponding Koutecky–Levich plots ( $J^{-1}$  versus  $\omega^{-0.5}$ ) at different potentials.



**Figure S5. Experiments with and without sacrificial reagents.** (a) DMPO spin trapping ESR technique to measure  $\bullet\text{O}_2^-$  over the CN-OH sample (reaction condition: 0.1 g/L of catalyst, ethanol : water = 9 : 1, irradiate for 2 min, 1 mM pBQ); (b) the effect of NBT for the photocatalytic  $\text{H}_2\text{O}_2$  production over the CN-OH sample (reaction conditions: 40 mg of catalyst, 25 mL of  $\text{H}_2\text{O}$ , 15 mL of ethanol, 5 mM of NBT, 300 W Xe lamp with a L42 cutoff filter,  $\lambda > 400$  nm); (c) colors of CN-OH in NBT solution before (left) and after (right) reaction.

**Table S6. pH values in solutions before and after reaction for the samples with different amounts of surface hydroxyl group**

	pH value (Before Reaction)	pH value (After Reaction)	Variation
CN	6.53±0.11	6.53±0.11	0.00
CN-OH-0.00	10.96±0.01	10.23±0.03	0.73
CN-OH-0.01	11.01±0.05	9.91±0.01	1.09
CN-OH-0.05	10.94±0.04	9.58±0.10	1.36

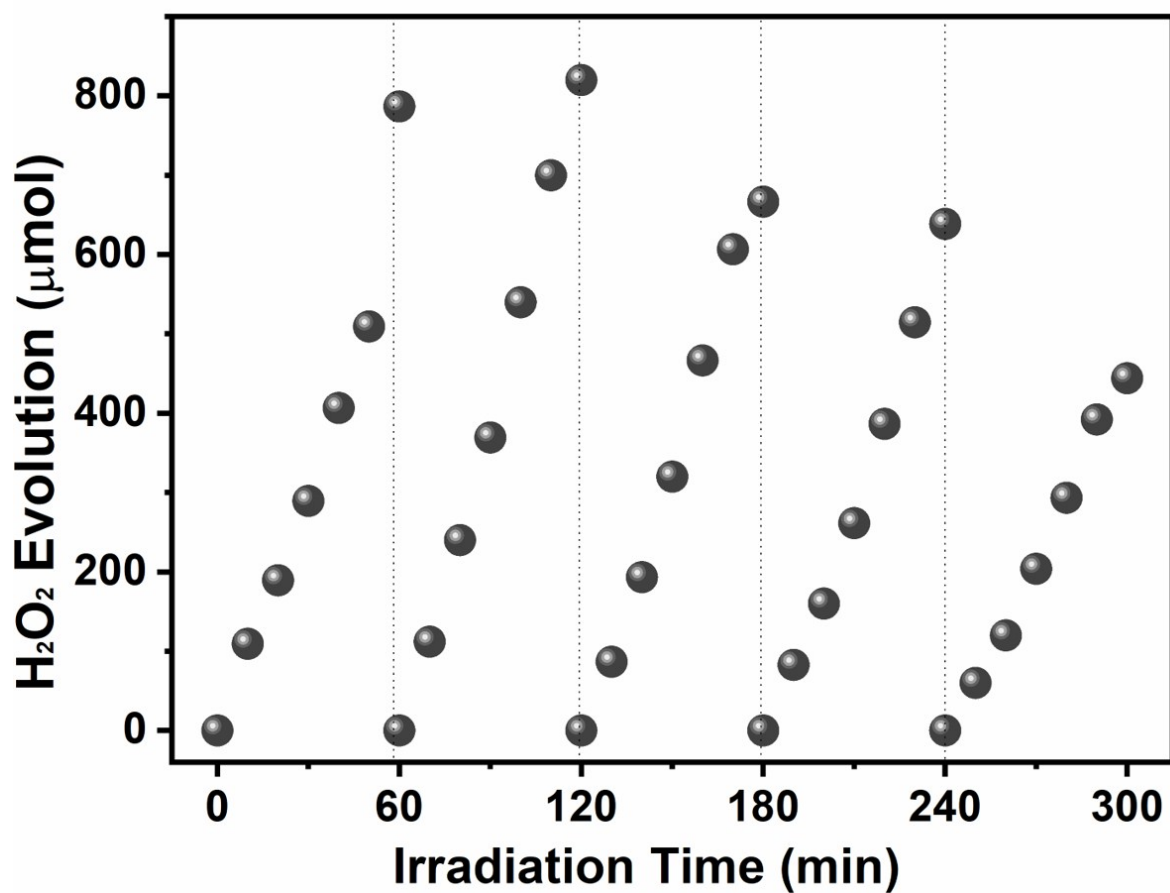
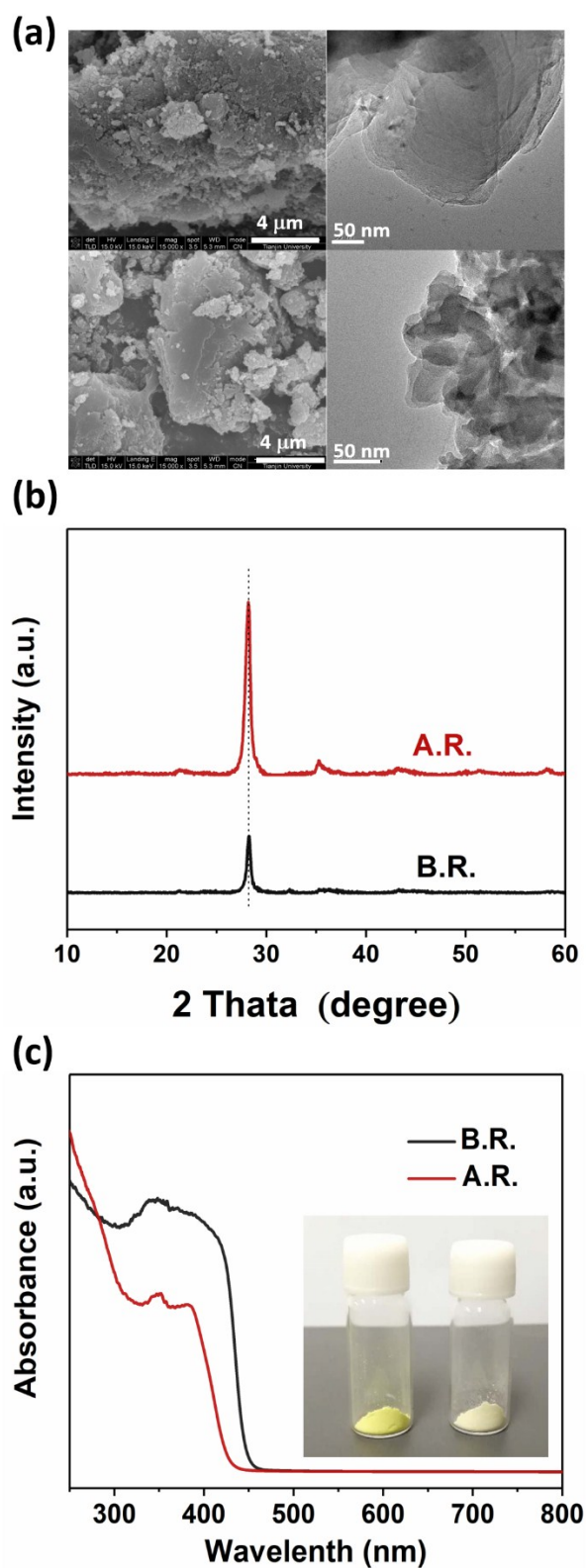


Figure S6. Cycle test of H<sub>2</sub>O<sub>2</sub> evolution over the CN-OH sample.



**Figure S7. Characterizations of the CN-OH sample before and after reaction.** (a) SEM (left), TEM (right) images of the CN-OH sample before (top) and after (bottom) reaction; (b) XRD patterns; (c) UV-visible absorption spectra of the CN-OH before and after reaction. (The inset of Fig. S6c are images of the sample before (left) and after (right) reaction).

**Table S7. pH values in solution of each cycle after reaction**

	1st	2nd	3rd	4th	5th
pH value	9.58	8.89	8.55	7.92	7.04

## References

- 1 H. Yu, R. Shi, Y. Zhao, T. Bian, Y. Zhao, C. Zhou, G.I.N. Waterhouse, L.Z. Wu, C.H. Tung and T. Zhang, *Adv. Mater.*, 2017, **29**, 1605148.
- 2 R.Wang, K. Pan, D. Han, J. Jiang, C. Xiang, Z. Huang, L. Zhang and X. Xiang, *ChemSusChem*, 2016, **9**, 2460-2469.
- 3 G.-h. Moon, M. Fujitsuka, S. Kim, T. Majima, X. Wang and W. Choi, *ACS Catal.*, 2017, **7**, 2886-2895.
- 4 Z. Wei, M. Liu, Z. Zhang, W. Yao, H. Tan and Y. Zhu, *Energy Environ. Sci.*, 2018, **11**, 2581-2589.
- 5 S. Zhao, X. Zhao, S. Ouyang and Y. Zhu, *Catal. Sci. Technol.* 2018, **8**, 1686-1695.
- 6 L. Shi, L. Yang, W. Zhou, Y. Liu, L. Yin, X. Hai, H. Song and J. Ye, *Small*, 2018, **14**, 1703142.
- 7 S. Kim, G.-h. Moon, H. Kim, Y. Mun, P. Zhang, J. Lee and W. Choi, *J. Catal.*, 2018, **357**, 51-58.